Long-Range Behavior of Noncovalent Bonds. Neutral and Charged H-Bonds, Pnicogen, Chalcogen, and Halogen Bonds

ARTICLE *in* CHEMICAL PHYSICS · APRIL 2015

Impact Factor: 1.65 · DOI: 10.1016/j.chemphys.2015.04.008

2 AUTHORS:

Binod Nepal

Utah State University

10 PUBLICATIONS **37** CITATIONS

SEE PROFILE

Steve Scheiner

Utah State University

366 PUBLICATIONS **11,197** CITATIONS

SEE PROFILE

Chemical Physics 456 (2015) 34–40

Contents lists available at ScienceDirect

Chemical Physics

journal homepage: www.elsevier.com/locate/chemphys

Long-range behavior of noncovalent bonds. Neutral and charged H-bonds, pnicogen, chalcogen, and halogen bonds

Binod Nepal, Steve Scheiner *

Department of Chemistry and Biochemistry, Utah State University, Logan, UT 84322-0300, United States

ARTICLE INFO

Article history:
Received 30 January 2015
In final form 15 April 2015
Available online 21 April 2015

Keywords:
Ab initio
MP2
SAPT
Electrostatic energy

ABSTRACT

Ab initio calculations show the drop in interaction energy with bond stretch ΔR can be fit to a common power n, in the functional form ΔR^{-n}. This exponent is smaller for charged H-bonds, as compared to neutral systems, where n varies in the order pnicogen < chalcogen < halogen bond. The decay is slowest for the electrostatic term, followed by induction and then by dispersion. The halogen bond has the greatest sensitivity to bond stretching in terms of all three components. The values of the exponent n are smaller for electrostatic energy than would be expected if it arose purely as a result of classical multipole interactions, such as dipole–dipole for the neutral systems. The exponents are larger when the fitting is done with respect to intermolecular distance R, rather than to its stretch relative to equilibrium length, although still not precisely matching what might be expected on classical grounds.

1. Introduction

Over the years, a great deal of information has accumulated regarding molecular interactions. Perhaps the most widely studied of these noncovalent forces is the hydrogen bond (HB), which embodies nearly a century of research [1–15] over the years. The HB was followed in ensuing years by examination of other related noncovalent bonds. The halogen bond, in which the bridging H is replaced by a halogen atom, was the next [16–29] in this chronology. While an attraction between a halogen and another electronegative atom seemed counterintuitive at first, it was realized that the partial negative charge around a halogen atom is quite anisotropic and contains positive as well as negative sub-regions. The electrostatic attraction is supplemented by a transfer of charge from the acceptor atom to the R–X σ^* antibonding orbital, where R represents any atom covalently attached to halogen X. The catalogue of noncovalent bonds was soon enlarged by the finding that the halogen can be replaced by other electronegative atoms, most particularly those of the chalcogen [30–40] and pnicogen [41–51] families.

The vast majority of information that has arisen about these various noncovalent bonds has been concerned with equilibrium geometries, those structures in which the donor and acceptor groups are situated fairly close to one another, where component attractive and repulsive forces balance one another. However, these interactions do not disappear when the two species begin to separate; they are merely weakened. The rate at which this weakening occurs has important implications. For example, if the noncovalent bond strength were to undergo only gradual decline, its effects would be important even if the two relevant groups were removed by fairly long separations. There is presumably a cutoff distance for each interaction, beyond which any lingering attractive forces are small enough to be comfortably ignored. But what is the cutoff for each sort of noncovalent bond, and how rapidly does the interaction energy approach this threshold? In a related question, what is the functional dependence of interaction energy on the separation distance R? The answers to these questions are especially important to the formulation of empirical functions designed to incorporate the effects of various noncovalent bonds into force fields that are used to simulate the dynamics of various systems.

In terms of explicit consideration of noncovalent bonds that are stretched well beyond their equilibrium separation, the H-bond has motivated a certain amount of limited study. In most cases, the interaction energy has been traced out, point by point, over a range of intermolecular distance. However, few of these studies extended this range of separation beyond 2 or 3 Å. Moreover, there have been scarce attempts to fit these points to a particular function, particularly at long range. There has been even less work in this direction addressing charged HBs, either cation-neutral or anion-neutral. And other noncovalent bonds, most notably the aforementioned halogen, chalcogen, and pnicogen bonds have been largely ignored [52] in terms of their long-range energetics.

* Corresponding author.
E-mail address: steve.scheiner@usu.edu (S. Scheiner).

http://dx.doi.org/10.1016/j.chemphys.2015.04.008
0301-0104/

The present work represents an attempt to fill in the existing gaps in our knowledge of the long-range behavior of the various sorts of noncovalent bonds. The neutral HB is compared to its ionic analogues, and these systems are then placed in the context of the halogen, chalcogen, and pnicogen bonds. The focus lies on the long range interaction, going out to as far as 11 Å stretched beyond the equilibrium separation. Attempts are made to ascertain which sort of function fits the computed binding energies at these long separations, and the results compared to what might be expected on simple physical grounds.

2. Theoretical methods

Calculations were carried out at the MP2/aug-cc-pVDZ level of theory, as implemented in the Gaussian-09 [53] software package. Each dimer was first fully optimized with no geometrical restraints. In order to examine the sensitivity to intermolecular separation, the optimized distance was stretched in fixed increments: 0.1 Å for the first 6 Å, and then 0.2 Å beyond that point. For each intermolecular distance, the remainder of the geometry was fully optimized. The binding energy at each point was computed as the difference between the energy of the heterodimer and the sum of energies of the isolated monomers, again fully optimized. This binding energy was corrected for basis set superposition error via the counterpoise procedure [54]. The interaction energy differs from the binding energy in that it is defined relative to the sum of the energies of the monomers when fixed in the geometry they adopt within the complex. The total interaction energy was dissected into various components by SAPT analysis using the MOLPRO [55] program. Kitaura-Morokuma energy decomposition was carried out using GAMESS [56]. Best fits of the energies to the intermolecular separation were analyzed via KaleidaGraph software.

3. Results

The fully optimized geometries of the heterodimers are illustrated in Figs. 1–4. Neutral H-bond pairs with OH, FH, and CH proton donors were considered. The bold numbers in Fig. 1 indicate the counterpoise-corrected binding energies which span a range from 1.8 kcal/mol for $F_3CH\cdots NH_3$ to 11.6 kcal/mol for $FH\cdots NH_3$. The HBs are considerably stronger, with binding energies as large as 41.2 kcal/mol, when an anion is used for proton acceptor, for systems pictured in Fig. 2. Very strong HBs are also associated with a cationic proton donor, as in the cases depicted in Fig. 3, considering both NH^+ and CH^+ donor groups. Recent work has focused attention on variants of HBs, where the bridging atom

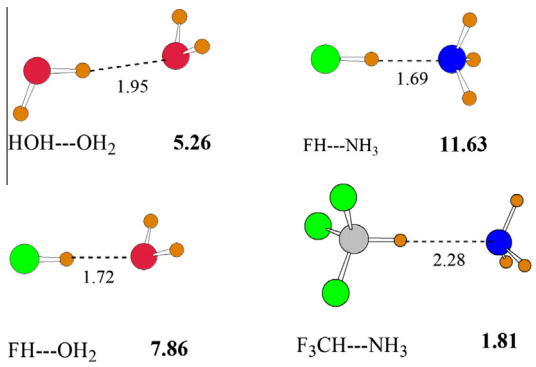

Fig. 1. Optimized geometries of neutral–neutral H-bonded complexes. The bold number indicates counterpoise-corrected binding energy in kcal/mol, distances in Å.

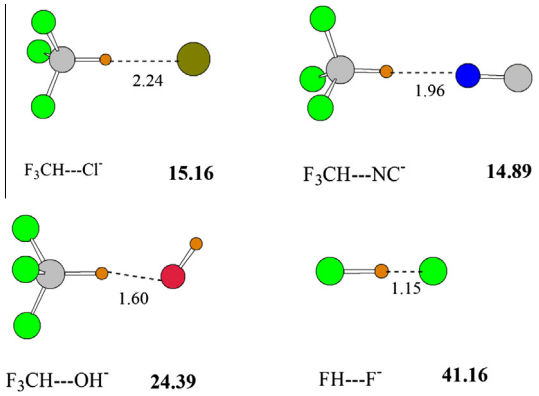

Fig. 2. Optimized geometries of anion-neutral H-bonded complexes. The bold number indicates counterpoise-corrected binding energy in kcal/mol, distances in Å.

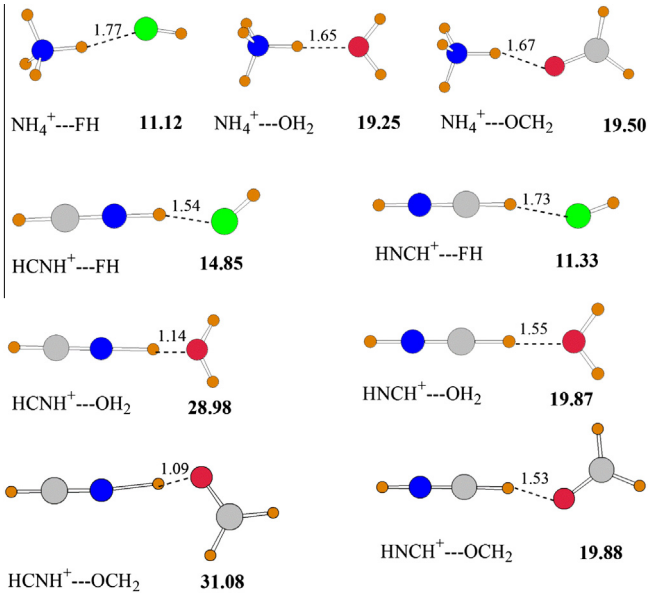

Fig. 3. Optimized geometries of cation-neutral H-bonded complexes. The bold number indicates counterpoise-corrected binding energy in kcal/mol, distances in Å.

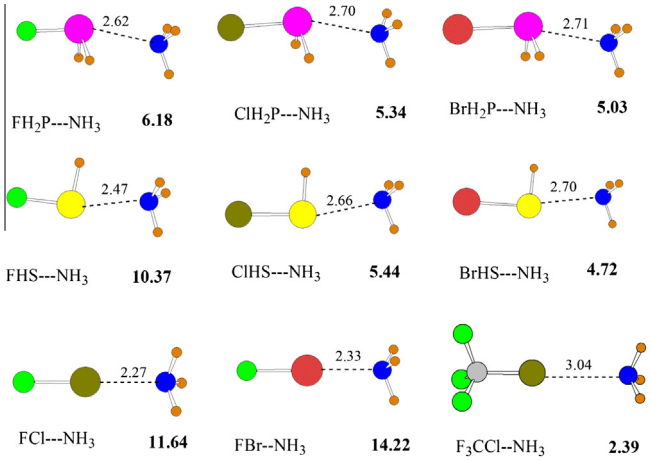

Fig. 4. Optimized geometries of pnicogen, chlacogen and halogen bonded complexes. The bold number indicates counterpoise-corrected binding energy in kcal/mol, distances in Å.

can be pnicogen, chalcogen, or halogen, which are the subject of the systems in Fig. 4. Such bonds can also be fairly strong, as for example FBr···NH_3 which has a binding energy of 14.2 kcal/mol.

Given the wide range of bond strengths in this diverse set of systems, and the interest in the manner, or speed, in which this bond is weakened by stretches, the energetics of stretching were normalized to one another. Specifically, each change in energy arising from a given bond stretch was divided by the full binding energy in the optimized dimer, i.e. the bold numbers in Figs. 1–4. The binding energy loss is thus represented as a percent of the full capacity of a given dimer. As an example, the percentage binding energy loss as the HB is stretched is shown for a set of six cationic HBs containing $HCNH^+$ in Fig. 5. It is immediately clear that the functional dependence of the binding energy percentage losses are quite similar, even though the binding energies themselves cover a wide range of 11–31 kcal/mol. The patterns are also relatively insensitive to whether it is the NH^+ or CH^+ end of the cation that serves as proton donor. This similarity is not limited to only this subset of systems, but is characteristic of all heterodimers, which may be seen in Fig. S1 in the Supplementary Information section.

The percentage bond energy decrease appears to be more or less linear in the first 1 Å of its stretch. A best fit of this quantity to a linear function in this range leads to a slope that characterizes the steepness of this energy loss. These slopes are reported in Table 1 where a number of patterns can be discerned. First with regard to neutral HBs, the slope is equal to 60 for conventional HBs HOH···OH_2, FH···NH_3, and FH···OH_2, but 10 units smaller for the CH···N HB in F_3CH···NH_3, suggesting a slightly more gradual die-off for the latter. The ionic HBs have a smaller slope than their neutral counterparts, in the range between 38 and 49. With the exception of FH···F^-, the anionic systems show a more gradual fall-off, but this may be a function of the CH donor. The slopes of the chalcogen-bonded systems are in line with those of the neutral HBs; pnicogen bonds fall more gradually, and halogen bonds more quickly. In fact, the halogen bond of FBr···NH_3 shows the largest slope and thus the most rapid loss of binding energy of any of the systems considered here.

As the binding energy loss levels off after the first Å stretch, a linear fit is no longer appropriate for longer intermolecular separations. A fitting was thus adjusted to an inverse ΔR^{-n} decay. That is, the exponent n was fit to the binding energy loss as R increases. No single value of n was appropriate for the entire range of stretching. Instead, this power was fit to individual spans of ΔR, terminating in ΔR = 11 Å. In other words, the best value of n was obtained for a range of ΔR from 1 Å to 11 Å. The same process was then undertaken for the 2–11 Å range, followed by 3–11 Å, and so on, terminating in the 10–11 Å range. These best-fit exponents n are listed in Table 2 for each set of systems. For example, this exponent is equal to 1.92 for the 1–11 Å range of the neutral HBs, as noted by the first entry in Table 2. The exponent rises to 2.10 for the 2–11 Å range, and so on, until reaching a maximal value of 2.52 for the furthest 10–11 Å range. Note that the values reported in Table 2 apply not to a single system, but are instead an average over several. The neutral HB set is thus an average of the four heterodimers in Fig. 1. (A breakdown of this data for the separate individual systems is available in Tables S1–S7.)

Table 1
The coefficients of linear function that fits the plots of % decrease of binding energy from optimal value vs. bond stretching in the region of 0–1 Å.

Complex	Coefficient	Complex	Coefficient
Neutral H-bonded complexes		Pnicogen bonded complexes	
H_2O···HOH	60.02	FH_2P···NH_3	54.39
FH···NH_3	59.64	ClH_2P···NH_3	51.08
H_2O···HF	61.37	BrH_2P···NH_3	50.82
F_3CH···NH_3	50.17		
Anion–neutral H-bonded complexes		Chalocogen bonded complexes	
F_3CH···Cl^-	37.58	FHS···NH_3	59.16
F_3CH···NC^-	39.58	ClHS···NH_3	57.17
F_3CH···OH^-	40.33	BrHS···NH_3	56.63
FH···F^-	48.21		
Cation–neutral H-bonded complexes		Halogen bonded complexes	
H_3N^+H···OH_2	46.47	FCl···NH_3	63.81
H_3N^+H···FH	40.20	FBr···NH_3	66.17
H_3N^+H···OCH_2	44.26	CF_3Cl···NH_3	58.72
HF···HNCH	49.40		
HF···HCNH	43.43		
H_2O···HNCH	44.14		
H_2O···HCNH	46.23		
HCHO···HNCH	42.87		
HCHO···HCNH	43.99		

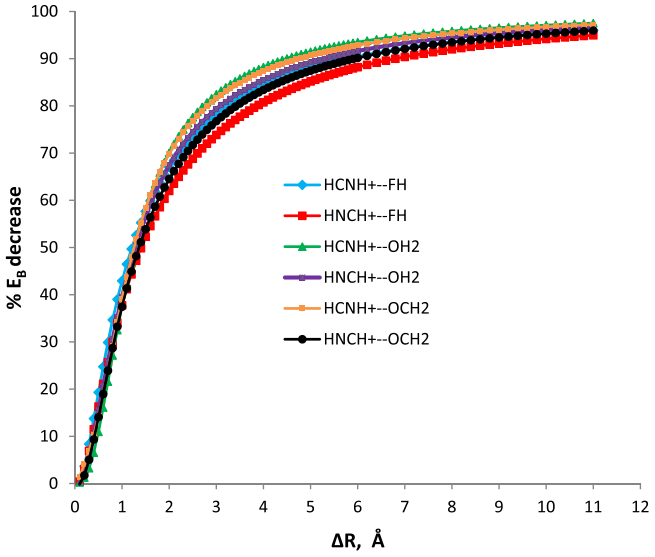

Fig. 5. Percent decrease of binding energy from the initial value vs. bond stretching for cation-neutral H-bonded complexes with $HCNH^+$ as proton donor.

The optimal values of power n are considerably smaller for the charged HBs in the next four columns of Table 2. The largest values are associated with the anionic systems, slightly larger than for the cationic HBs. Note that these quantities are consistently larger for the NH end of $HCNH^+$ than for the CH end. Like the short-range behavior described in Table 1, the powers of n for the other sorts of bonds vary as pnicogen < chalcogen < halogen bond, again indicating a faster fall-off of binding energy for the latter system, this time for long range.

The quantities in Table 2 may perhaps be more readily understood when compared graphically as in Fig. 6. The larger values of n for the neutral as compared to ionic systems are immediately apparent. Also evident is the order of pnicogen < chalcogen < halogen bond; the neutral HBs are generally similar to the pnicogen bonds. The slightly larger values of n for the anionic, compared to cationic, is also clear in Fig. 6, as is the smaller values for CH^+ compared to NH^+.

Although appearing to be reaching for an asymptote, the curves in Fig. 6 have not yet reached a point where they are no longer changing. One might anticipate that at very long range, the only sort of interaction still present is electrostatic. For a pair of neutrals, the largest lingering quantity at this distance would correspond to a dipole–dipole interaction, which classically dies off as R^{-3}. While the curves in the upper part of Fig. 6 have not yet attained this value, a power of −3 does appear to be their asymptote. Likewise, the charged systems in the lower part of

Table 2
Average exponents n of the power functions ΔR^{-n} that fit the plots of binding energy vs. bond stretching at different ranges for non-covalent complexes.

Range Å	H-bond neutral–neutral	H-bond anion-neutral	H-bond cation-neutral (NH_4^+ donor)	H-bond cation-neutral ($HCNH^+$) NH-donor	H-bond cation-neutral ($HCNH^+$) CH-donor	Pnicogen bond	Chalcogen bond	Halogen bond
1–11	1.92	1.31	1.16	1.30	1.18	2.01	2.10	2.23
2–11	2.10	1.43	1.27	1.38	1.28	2.16	2.28	2.39
3–11	2.20	1.49	1.34	1.44	1.35	2.24	2.37	2.48
4–11	2.26	1.52	1.39	1.47	1.39	2.29	2.42	2.53
5–11	2.32	1.56	1.43	1.50	1.43	2.34	2.47	2.56
6–11	2.39	1.62	1.50	1.53	1.47	2.38	2.51	2.60
7–11	2.44	1.65	1.54	1.55	1.49	2.41	2.54	2.62
8–11	2.47	1.66	1.56	1.57	1.51	2.43	2.56	2.63
9–11	2.49	1.68	1.59	1.58	1.52	2.45	2.58	2.65
10–11	2.52	1.69	1.61	1.60	1.54	2.47	2.60	2.66

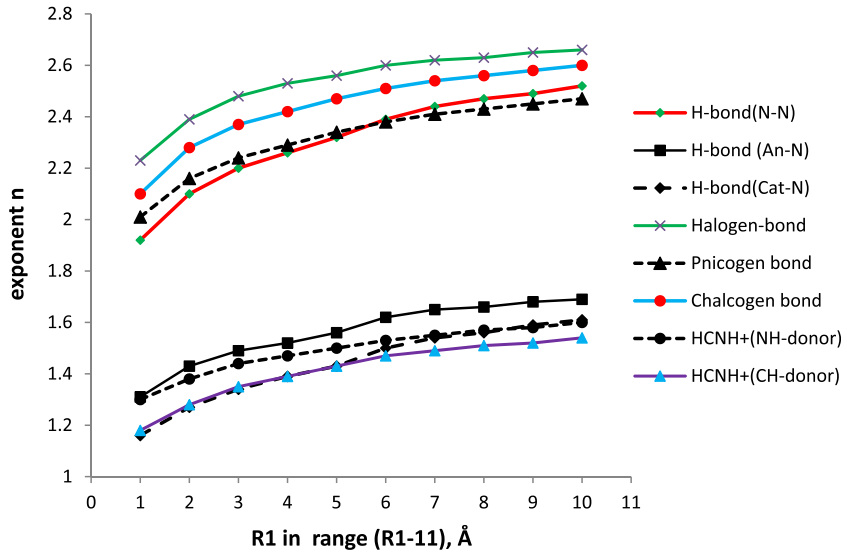

Fig. 6. Average exponent n of power function $(\Delta R)^{-n}$ vs. range of bond stretching for various complexes. Each value on the x-axis indicates lower value R_1 of the $(R_1–11)$ Å range.

Fig. 6 ought to be striving toward a charge–dipole interaction at very long range, which should have a power dependence of −2. In any case, the exponents for the charged systems are roughly 1 unit smaller than those of the neutral dimers.

3.1. Energy decomposition

The total interaction energy of complexes such as these encompasses a number of different components. The exchange repulsion is expected to be of very short range, dying off very quickly as the electron clouds of the two subunits disengage from one another. Only slightly longer range would be dispersion attraction, typically considered to die off roughly as R^{-6}. Induction energy wherein the charge distributions of each molecule perturb the electron cloud of its partner, should extend a bit further out. The longest range interaction is anticipated to be electrostatic.

Each of these components can be evaluated separately within the framework of SAPT decomposition. The distance dependence of each component is displayed as an example in Fig. 7 for three of the cationic H-bonded systems. Again, each term is normalized, as a percentage of its value in the equilibrium geometry, so as to maximize the ability for comparison. Fig. 7c illustrates the very rapid decay of the dispersion attraction, losing nearly all of its value in the first 2 Å of stretch. It may also be noted that the manner of dispersion energy loss is independent of the particular proton donor, as the three curves in Fig. 7c coincide. Induction energy loss is also rapid, albeit not as abrupt, as is evident in Fig. 7b. The drop in induction energy is slightly steeper for the $HCNH^+$ donor than for $HNCH^+$ or NH_4^+. The much slower decay of the electrostatic energy is evident in Fig. 7a. A stretch of some 6 Å is required before this attractive term is diminished by 90%. As in the case of induction, there is a slightly less gradual drop-off of electrostatic energy for $HCNH^+$ than for $HNCH^+$ or NH_4^+. Exchange repulsion is not explicitly displayed as its very short-range character led to its disappearance for stretches beyond 1 Å. The data for the individual systems are listed in Table S8 and illustrated in Figs. S2–S6 of the Supplementary Information, and are quite similar.

As was done earlier for the total interaction energy, each individual component can be fit to a function that dies off as ΔR^{-n}, and the value of n extracted for each region of stretch ΔR. These powers can be grouped into regions. In this case, the short range is defined as stretches between 1 and 5 Å, and long range as 5–11 Å. These powers are reported in Tables 3 and 4 for each of the heterodimers under consideration, with average values displayed in the last row of each section.

For example, the uppermost section of Table 3 indicates that the electrostatic component of the neutral HBs, as a group, decays as $\Delta R^{-1.53}$ between 1 and 5 Å, and then as $\Delta R^{-2.41}$ for the 5–11 Å range. The powers are considerably larger for induction and dispersion, indicating their more rapid decline with ΔR. Comparison with the charged HBs in the next two sections indicates the dispersion exponents are little changed by addition of a charge. Induction

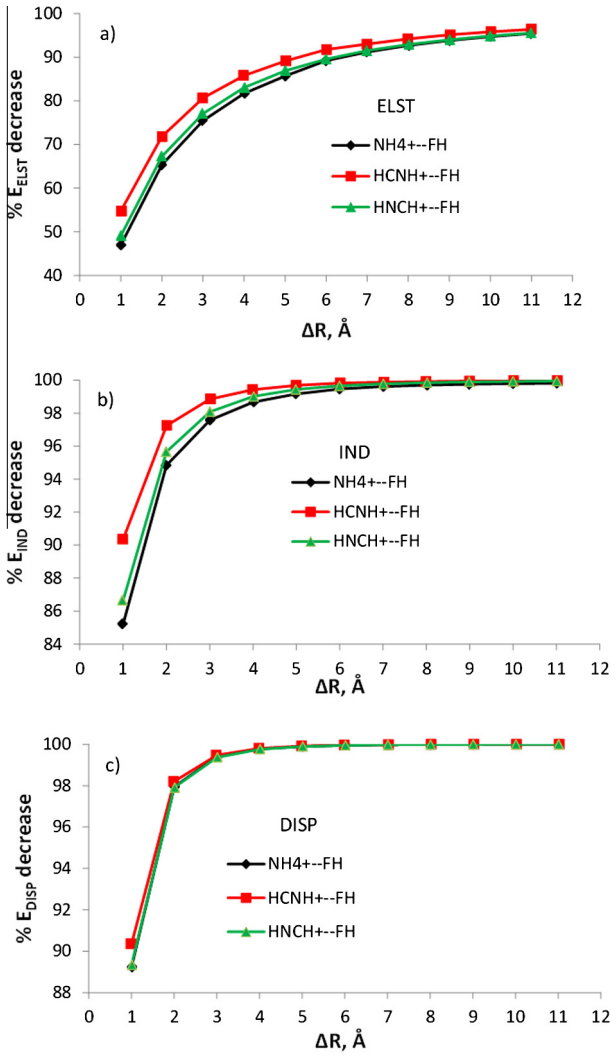

Fig. 7. Percent decrease of (a) electrostatic (ELST), (b) induction (IND) and (c) dispersion (DISP) components from their equilibrium values due to bond stretching for cation-neutral H-bonded complexes.

Table 3
The exponent values n of the functions ΔR^{-n} that fit the plots of different components of the binding energy (electrostatic, induction, and dispersion) vs. the bond stretching for different H-bonded complexes in different ranges.

Complex	ELST			IND			DISP		
	1–5	1–11	5–11	1–5	1–11	5–11	1–5	1–11	5–11
Neutral–neutral H-bonded complexes									
FH···OH_2	1.53	1.85	2.33	3.33	3.83	4.63	3.13	3.68	4.53
H_2O···HOH	1.40	1.65	2.43	3.30	3.48	4.38	2.98	3.50	4.39
FH···NH_3	1.79	2.11	2.58	3.78	4.25	4.97	3.34	3.92	4.75
F_3CH···NH_3	1.41	1.75	2.28	2.91	3.49	4.41	2.70	3.27	4.15
Average	1.53	1.84	2.41	3.33	3.76	4.60	3.04	3.59	4.46
Anion–neutral H-bonded complexes									
F_3CH···Cl^-	0.92	1.13	1.49	1.94	2.28	2.89	2.88	3.40	4.31
F_3CH···NC^-	0.92	1.13	1.44	1.84	2.21	2.79	2.76	3.30	4.14
F_3CH···OH^-	1.10	1.29	1.60	2.30	2.58	3.07	3.22	3.81	4.60
FH···F^-	1.22	1.41	1.67	2.62	2.87	3.26	3.76	4.27	4.90
Average	1.04	1.24	1.55	2.18	2.49	3.00	3.16	3.70	4.49
Cation-neutral H-bonded complexes									
H_3NH^+···FH	0.81	1.06	1.43	1.87	2.29	2.94	2.88	3.51	4.51
$HCNH^+$···FH	0.88	1.08	1.37	2.10	2.43	2.89	2.92	3.48	4.25
$HNCH^+$···FH	0.84	1.05	1.37	1.95	2.32	2.89	2.85	3.40	4.25
Average	0.84	1.06	1.39	1.97	2.35	2.91	2.88	3.46	4.34

exponents, however, are considerably smaller, indicating that the charge on one subunit or the other leads to a slower decay of this component. Likewise, the ELST exponents also drop with the introduction of charge, particularly for the 5–11 Å range. The exponents for the other neutral complexes in Table 4 are generally similar to the neutral HBs. Overall, these exponents rise slightly in the order pnicogen < chalcogen < halogen-bonded, consistent with the pattern noted earlier for the total interaction energy. Indeed, among all types of noncovalent interactions, the halogen bond has the greatest sensitivity to bond stretching in terms of all three components. The average exponent for electrostatic, induction, and dispersion energies are 1.78/2.46, 3.86/4.60 and 2.90/4.38, respectively, for the 1–5 Å/5–11 Å regions.

4. Discussion

The calculations described here made use of the polarized double-ζ aug-cc-pVDZ basis set. The latter is obviously not the largest basis set one can envision. Larger sets would likely enlarge dispersion energy which tends to correlate with basis set size. Electrostatic and induction components would also change, albeit in a less predictable manner, as the basis set is expanded. However, the emphasis in this work is not on the computation of highly accurate numerical values for each term, but rather the functional dependence of how quickly each diminishes as the participating units are separated from one another. It is not expected that this functional dependence will be very sensitive to basis set size, provided the set is well balanced, and includes polarization and diffuse functions. Moreover, it is reiterated that a large portion of the error arising from deficiencies in the basis set were alleviated by the application of counterpoise correction.

Similar considerations apply to the MP2 treatment of electron correlation. Again, higher orders of perturbation theory would have likely resulted in somewhat different magnitudes of correlation energy, as would other means of computing this quantity, e.g. CCSD(T). But the MP2 treatment ought to provide a relatively accurate portrayal of the way in which correlation affects the rapidity with which each term is diminished with intermolecular separation, which is at the heart of this work. Moreover, this procedure takes on added importance as it represents the most widely used ab initio procedure to evaluate electron correlation at the present time. (DFT includes correlation as well, but is not an ab initio method.) Accordingly, knowledge of the functional dependence of

Table 4
The exponent values n of the functions ΔR^{-n} that fit the plots of different components of the binding energy (electrostatic, induction, and dispersion) vs. the bond stretching for pnicogen, chalcogen and halogen-bonded complexes.

Complex	ELST			IND			DISP		
	1–5	1–11	5–11	1–5	1–11	5–11	1–5	1–11	5–11
Pnicogen-bonded complexes									
FH_2P···NH_3	1.58	1.85	2.26	3.42	3.80	4.48	2.86	3.47	4.39
ClH_2P···NH_3	1.57	1.83	2.24	3.34	3.71	4.40	2.82	3.40	4.29
BrH_2P···NH_3	1.55	1.81	2.23	3.29	3.67	4.37	2.79	3.37	4.25
Average	1.57	1.83	2.24	3.35	3.73	4.42	2.82	3.41	4.31
Chalcogen-bonded complexes									
FHS···NH_3	1.69	1.95	2.36	3.81	4.00	4.58	2.99	3.57	4.45
ClHS···NH_3	1.62	1.91	2.36	3.45	3.80	4.45	2.82	3.39	4.26
BrHS···NH_3	1.62	1.92	2.38	3.38	3.74	4.40	2.77	3.34	4.20
Average	1.64	1.93	2.37	3.55	3.85	4.48	2.86	3.43	4.30
Halogen-bonded complexes									
FCl···NH_3	1.89	2.15	2.56	4.16	4.34	4.80	3.06	3.66	4.58
FBr···NH_3	1.89	2.13	2.50	4.35	4.43	4.72	3.06	3.64	4.50
CF_3Cl···NH_3	1.56	1.86	2.32	3.06	3.51	4.29	2.57	3.15	4.06
Average	1.78	2.05	2.46	3.86	4.09	4.60	2.90	3.48	4.38

interaction energy is important as it affects the calculation of a large number of intermolecular contacts.

There might have been an initial expectation that the long-range behavior of these various noncovalent bonds ought to be dominated by electrostatic terms. This does in fact seem to be the case, as the exponents that characterize the die-off of the ELST term are considerably smaller than those for induction and dispersion. Taking the pnicogen-bonded systems as an example, the average exponent in the ΔR = 5–11 Å range is 2.24, as compared to values of 4.42 and 4.31 for IND and DISP, respectively. ELST and IND drop less precipitously for the charged systems. In the case of the cation-neutral HBs, their respective exponents in the same range are 1.39 and 2.91. Dispersion energy, on the other hand, is little affected by placing a charge on one of the two subunits.

Further, focusing on the ELST component, it would be logical to presume that the long-range electrostatics of the neutral systems ought to reduce to a dipole–dipole interaction, which classically dies off as R^{-3}. However, a glance at the data in Tables 3 and 4 indicates the best-fit exponent for the ELST term is smaller than 3 for the neutral pairs, between 2.2 and 2.5. It would appear then that the long-range behavior of the Coulombic attraction cannot be accurately reduced to a simple R^{-3} charge–dipole function. Along similar lines, a R^{-2} dependence might have been anticipated for the charge–dipole interaction of the charged HBs. The long-range ELST exponent for the charged HBs are 1.4 for the cation and 1.6 for the anion, somewhat smaller than the expected value.

Basis set superposition is a recognized source of error in supermolecule calculations of the sort that have been applied to evaluate binding energies in these complexes. Of course, these errors dwindle quickly as the two subunits are distanced from one another, and are not a source of concern for long-range behavior. On the other hand, it is worth considering how this error affects the equilibrium geometries and energetics. Geometries of the various complexes were reoptimized with counterpoise corrections included directly at each step of the optimization. The changes in the H-bond length R and the H-bond angle θ displayed in the first two columns of Table S9 show that inclusion of counterpoise alters equilibrium geometries by only a small amount. The intermolecular distance increases by 0.1 Å or less, and the angle remains within a degree of its uncorrected value, with the exception of a 4° change for $H_3N^+H\cdots FH$. Most importantly, these minor geometrical alterations have virtually no effect upon the binding energies. As shown in the third column of Table S9, the reoptimization causes only minute changes in E_b, less than 0.1 kcal/mol. And even these minor effects will be reduced quickly as the two subunits are moved away from one another, especially in the long range which is the focus of this work. The total magnitudes of the basis set superposition error, as evaluated via the counterpoise procedure, are displayed in the last two columns of Table S9, at both the corrected and uncorrected equilibrium geometries. The counterpoise correction of the geometry has only very small effects on this quantity as well.

It is well known that any scheme for partitioning the total interaction energy is arbitrary to some degree. It would hence be wise to compare the SAPT values to those computed using a different scheme. The Kitaura–Morokuma (KM) energy partitioning method [57–59] is one of the first devised and has witnessed extensive use over the years, and has demonstrated its usefulness and validity. The KM values of the ES and EX energies are displayed in Table S10 alongside the SAPT quantities for the equilibrium geometries of the indicated complexes. In most cases, the values computed by the two methods are very similar indeed. For example, the two ES values are within 0.1 kcal/mol of one another for the $F_3CH\cdots Cl^-$ complex, and the EX quantities within 0.2 kcal/mol. The SAPT and KM values of ES differ by 0.2 kcal/mol on average, and the EX energies are within 0.5 kcal/mol. While the physical meanings of ES and EX are reasonably similar for KM and SAPT, the second-order quantities are quite different. The SAPT induction energy IND is very roughly analogous to the summation of KM polarization (POL) and charge transfer (CT) energies. The last two columns of Table S10 indicate that despite these different definitions, the two partitioning procedures nevertheless yield fairly similar values in most cases. These similarities of the various components lend confidence that the conclusions discussed above for the SAPT analysis would likely be confirmed for other energy decomposition schemes as well.

It might also be stressed that any energy decomposition scheme, and SAPT is no exception, can begin to break down as the two subunits come very close together, and the interaction energy climbs. It is thus reassuring that the KM and SAPT components are as similar as they are even for the most strongly bound complexes, where one subunit carries a charge. For example, the KM and SAPT values of the electrostatic energy for the $FH\cdots F^-$ complex are −74.96 and −75.01 kcal/mol, respectively. Perhaps more importantly, the emphasis here is placed on the long-range behavior, where the SAPT procedure is most trustworthy.

By considering the percent drops in energetic quantities and the stretches of each intermolecular distance from its equilibrium value, the behaviors of the various systems have been normalized to one another which allows direct comparisons to be made between one complex and another, unifying all the different types of H-bonds: strong and weak, and short and long. However, one might also be interested in the raw data itself. That is one might consider correlations between the unnormalized binding energies and the intermolecular distances R, rather than the stretch from equilibrium. In particular, R is defined as the distance between the electron donor and acceptor atoms.

The fitting of E_b to R for the various systems is reported in Tables S11–S17, corresponding to the fits to ΔR in the earlier tables. The patterns are generally similar with two exceptions. First, while the exponents characterizing ΔR^{-n} tend to increase as the range covered expands to longer stretches, the R^{-n} exponents show a tendency to become slightly smaller. Second, the exponents n for the fit to R^{-n} are somewhat larger than those for ΔR^{-n}. Taking the average of the neutral HBs as an example, n reaches 2.52 for the stretching region of ΔR = 10–11 Å; the exponent is 3.19 for R. This behavior characterizes all of the neutral systems, whether H-bonding, or halogen, chalcogen, or pnicogen: n is smaller than 3 for ΔR and larger for R. Similarly for the anionic HBs where n is less than 2 for ΔR, and is slightly larger than 2 for R. In the case of the cationic HBs, the exponents are closer to 2.0 for the fit of E_b to R.

With regard to the individual components, the fits to R also provide larger exponents than do those for ΔR^{-n}. As indicated earlier in Table 3, the exponents n for the electrostatic component fit to ΔR^{-n} are 2.4, 1.6, and 1.4 for the neutral, anionic, and cationic HBs, respectively. When fit instead to the actual intermolecular distance R, these exponents rise to the larger values of 3.2, 2.1, and 1.9, as indicated in Table S18. Likewise for the pnicogen, chalcogen, and halogen-bonded systems where these ΔR^{-n} exponents are in the range 2.2–2.5, and those for R^{-n} are between 3.1 and 3.2 (Table S19). Similar increases are observed also for the induction and dispersion components. The ΔR^{-n} exponents for the neutral systems for the induction energy are 4.4–4.6, compared to 6.0–6.3 for R^{-n}; the corresponding exponents are 2.9–3.0 and 4.0–4.1 for the ionic complexes. The rate of dispersion die-off is relatively insensitive to charge; it diminishes as $\Delta R^{-4.4}$ whereas it is more variable for R, with exponents varying between 5.7 and 6.1. In summary, when fit to R (Table S20), the electrostatic exponents are closer to the values of 3 and 2 normally expected for neutral and charged dimers, respectively, even if a little larger; likewise for the R^{-6} die-off of the dispersion energy.

Conflict of interest

None declared.

Acknowledgments

Computer, storage and other resources from the Division of Research Computing in the Office of Research and Graduate Studies at Utah State University are gratefully acknowledged.

Appendix A. Supplementary data

Supplementary data associated with this article can be found, in the online version, at http://dx.doi.org/10.1016/j.chemphys.2015.04.008.

References

[1] R.M. Badger, S.H. Bauer, J. Chem. Phys. 5 (1939) 839.
[2] G.C. Pimentel, A.L. McClellan, The Hydrogen Bond, Freeman, San Francisco, 1960.
[3] M.D. Joesten, L.J. Schaad, Hydrogen Bonding, Marcel Dekker, New York, 1974.
[4] P. Schuster, G. Zundel, C. Sandorfy (Eds.), The Hydrogen Bond. Recent Developments in Theory and Experiments, North-Holland Publishing Co., Amsterdam, 1976.
[5] E.N. Baker, R.E. Hubbard, Prog. Biophys. Mol. Biol. 44 (1984) 97.
[6] Z. Latajka, S. Scheiner, J. Chem. Phys. 87 (1987) 5928.
[7] G.A. Jeffrey, W. Saenger, Hydrogen Bonding in Biological Structures, Springer-Verlag, Berlin, 1991.
[8] S. Scheiner, in: Z.B. Maksic (Ed.), Theoretical Models of Chemical Bonding, Springer-Verlag, Berlin, 1991, p. 171.
[9] S. Scheiner, Hydrogen Bonding. A Theoretical Perspective, Oxford University Press, New York, 1997.
[10] S. Scheiner, in: Z.B. Maksic, W.J. Orville-Thomas (Eds.), Pauling's Legacy – Modern Modelling of the Chemical Bond, Elsevier, Amsterdam, 1997, p. 571.
[11] G.R. Desiraju, T. Steiner, The Weak Hydrogen Bond in Structural Chemistry and Biology, Oxford, New York, 1999.
[12] Y. Gu, T. Kar, S. Scheiner, J. Mol. Struct. 552 (2000) 17.
[13] S.J. Grabowski (Ed.), Hydrogen Bonding – New Insights, Springer, Dordrecht, 2006.
[14] S. Scheiner, L. Wang, J. Am. Chem. Soc. 115 (1993) 1958.
[15] G. Gilli, P. Gilli, The Nature of the Hydrogen Bond, Oxford University Press, Oxford, UK, 2009.
[16] O. Hassel, Science 170 (1970) 497.
[17] S.C. Blackstock, J.P. Lorand, J.K. Kochi, J. Org. Chem. 52 (1987) 1451.
[18] N. Ramasubbu, R. Parthasarathy, P. Murray-Rust, J. Am. Chem. Soc. 108 (1986) 4308.
[19] J.P.M. Lommerse, A.J. Stone, R. Taylor, F.H. Allen, J. Am. Chem. Soc. 118 (1996) 3108.
[20] P. Auffinger, F.A. Hays, E. Westhof, P.S. Ho, Proc. Nat. Acad. Sci. USA 101 (2004) 16789.
[21] P. Politzer, P. Lane, M.C. Concha, Y. Ma, J.S. Murray, J. Mol. Model. 13 (2007) 305.
[22] A. Karpfen, in: P. Metrangolo, G. Resnati (Eds.), Halogen Bonding, Fundamentals and Applications, Springer, Berlin, 2008, p. 1.
[23] P. Metrangolo, G. Resnati, Halogen Bonding. Fundamentals and Applications, Springer, Berlin, 2008.
[24] K. Eskandari, H. Zariny, Chem. Phys. Lett. 492 (2010) 9.
[25] A.C. Legon, Phys. Chem. Chem. Phys. 12 (2010) 7736.
[26] M. Erdelyi, Chem. Soc. Rev. 41 (2012) 3547.
[27] S.J. Grabowski, Chem. Phys. Lett. 605–606 (2014) 131.
[28] C. Wang, D. Danovich, Y. Mo, S. Shaik, J. Chem. Theory Comput. 10 (2014) 3726.
[29] A. Mukherjee, S. Tothadi, G.R. Desiraju, Acc. Chem. Res. 47 (2014) 2514.
[30] R.E. Rosenfield, R. Parthasarathy, J.D. Dunitz, J. Am. Chem. Soc. 99 (1977) 4860.
[31] T.N.G. Row, R. Parthasarathy, J. Am. Chem. Soc. 103 (1981) 477.
[32] M. Iwaoka, S. Takemoto, S. Tomoda, J. Am. Chem. Soc. 124 (2002) 10613.
[33] F.T. Burling, B.M. Goldstein, J. Am. Chem. Soc. 114 (1992) 2313.
[34] W. Wang, B. Ji, Y. Zhang, J. Phys. Chem. A 113 (2009) 8132.
[35] U. Adhikari, S. Scheiner, J. Phys. Chem. A 118 (2014) 3183.
[36] L.M. Azofra, S. Scheiner, J. Phys. Chem. A 118 (2014) 3835.
[37] V.d.P.N. Nziko, S. Scheiner, J. Phys. Chem. A 118 (2014) 10849.
[38] X. Guo, Y.-W. Liu, Q.-Z. Li, W.-Z. Li, J.-B. Cheng, Chem. Phys. Lett. 620 (2015) 7.
[39] L.M. Azofra, I. Alkorta, S. Scheiner, Phys. Chem. Chem. Phys. 16 (2014) 18974.
[40] L.M. Azofra, S. Scheiner, J. Chem. Phys. 140 (2014) 034302.
[41] K.W. Klinkhammer, P. Pyykko, Inorg. Chem. 34 (1995) 4134.
[42] J.S. Murray, P. Lane, P. Politzer, Int. J. Quantum Chem. 107 (2007) 2286.
[43] J. Moilanen, C. Ganesamoorthy, M.S. Balakrishna, H.M. Tuononen, Inorg. Chem. 48 (2009) 6740.
[44] S. Scheiner, J. Chem. Phys. 134 (2011) 094315.
[45] U. Adhikari, S. Scheiner, J. Chem. Phys. 135 (2011) 184306.
[46] S. Zahn, R. Frank, E. Hey-Hawkins, B. Kirchner, Chem. Eur. J. 17 (2011) 6034.
[47] S. Scheiner, U. Adhikari, J. Phys. Chem. A 115 (2011) 11101.
[48] J.E. Del Bene, I. Alkorta, J. Elguero, J. Phys. Chem. A 119 (2014) 224.
[49] S. Scheiner, Acc. Chem. Res. 46 (2013) 280.
[50] S. Sarkar, M.S. Pavan, T.N. Guru Row, Phys. Chem. Chem. Phys. 17 (2015) 2330.
[51] G. Sánchez-Sanz, C. Trujillo, I. Alkorta, J. Elguero, Theor. Chem. 1053 (2015) 305.
[52] S. Scheiner, Cryst. Eng. Commun. 15 (2013) 3119.
[53] M.J. Frisch, G.W. Trucks, H.B. Schlegel, G.E. Scuseria, M.A. Robb, J.R. Cheeseman, G. Scalmani, V. Barone, B. Mennucci, G.A. Petersson, H. Nakatsuji, M. Caricato, X. Li, H.P. Hratchian, A.F. Izmaylov, J. Bloino, G. Zheng, J.L. Sonnenberg, M. Hada, M. Ehara, K. Toyota, R. Fukuda, J. Hasegawa, M. Ishida, T. Nakajima, Y. Honda, O. Kitao, H. Nakai, T. Vreven, J.A. Montgomery, J.E. Peralta, F. Ogliaro, M. Bearpark, J.J. Heyd, E. Brothers, K.N. Kudin, V.N. Staroverov, T. Keith, R. Kobayashi, J. Normand, K. Raghavachari, A. Rendell, J.C. Burant, S.S. Iyengar, J. Tomasi, M. Cossi, N. Rega, J.M. Millam, M. Klene, J.E. Knox, J.B. Cross, V. Bakken, C. Adamo, J. Jaramillo, R. Gomperts, R.E. Stratmann, O. Yazyev, A.J. Austin, R. Cammi, C. Pomelli, J.W. Ochterski, R.L. Martin, K. Morokuma, V.G. Zakrzewski, G.A. Voth, P. Salvador, J.J. Dannenberg, S. Dapprich, A.D. Daniels, O. Farkas, J.B. Foresman, J.V. Ortiz, J. Cioslowski, D.J. Fox, Gaussian 09. Gaussian, Inc, Wallingford CT, 2009.
[54] S.F. Boys, F. Bernardi, Mol. Phys. 19 (1970) 553.
[55] H.-J. Werner, P.J. Knowles, F.R. Manby, M. Schütz, P. Celani, G. Knizia, T. Korona, R. Lindh, A. Mitrushenkov, G. Rauhut, T.B. Adler, R.D. Amos, A. Bernhardsson, A. Berning, D.L. Cooper, M.J.O. Deegan, A.J. Dobbyn, F. Eckert, E. Goll, C. Hampel, A. Hesselmann, G. Hetzer, T. Hrenar, G. Jansen, C. Köppl, Y. Liu, A.W. Lloyd, R.A. Mata, A.J. May, S.J. McNicholas, W. Meyer, M.E. Mura, A. Nicklaß, P. Palmieri, K. Pflüger, R. Pitzer, M. Reiher, T. Shiozaki, H. Stoll, A.J. Stone, R. Tarroni, T. Thorsteinsson, M. Wang, A. Wolf, MOLPRO, 2010.
[56] M.W. Schmidt, K.K. Baldridge, J.A. Boatz, S.T. Elbert, M.S. Gordon, J.H. Jensen, S. Koseki, N. Matsunaga, K.A. Nguyen, S. Su, T.L. Windus, M. Dupuis, J.A. Montgomery, J. Comput. Chem. 14 (1993) 1347.
[57] K. Kitaura, K. Morokuma, Int. J. Quantum Chem. 10 (1976) 325.
[58] K. Morokuma, K. Kitaura, in: P. Politzer, D.G. Truhlar (Eds.), Chemical Applications of Atomic and Molecular Electrostatic Potentials, Plenum, New York, 1981, p. 215.
[59] K. Morokuma, K. Kitaura, in: H. Ratajczak, W.J. Orville-Thomas (Eds.), Molecular Interactions, Wiley, New York, 1980, p. 21.